ORIGINAL RESEARCH **Open access**

Early Detection of Water Stress in Lettuce Using Thermal Infrared and RGB Image Fusion

Mikko Lahtinen[1*], Elina Salo[1], Juhani Virtanen[2], Hanna Mäkelä[3], Kari Lehtonen[1], Sanna Nieminen[2]

Abstract

Identifying water stress early is essential to maximize water productivity and ensuring long-term sustainability. Conventional Internet of Things (IoT) tools, such as soil moisture detectors, often fall short of delivering prompt notifications, leading to wasteful irrigation and, at times, crop damage. This study presents a novel technique for early recognition of water stress in lettuce, using Thermal Infrared (TIR) and RGB imaging in a controlled laboratory environment. The introduced methodology combines sophisticated image analysis procedures, including background removal through Hue-Saturation-Value (HSV) thresholding, wavelet-based denoising to refine thermal pictures, integration of RGB and TIR via Principal Component Analysis (PCA), and Gaussian Mixture Model (GMM) clustering to isolate stressed zones. Affected leaf regions are indicated on the RGB image using yellow false coloring. This strategy rests on the understanding that stomatal closure diminishes transpiration, thereby elevating the temperature of the impacted tissue. Experimental outcomes show that this new strategy can recognize water stress up to 84 h earlier than standard soil moisture gauges. Additionally, a comparative investigation was conducted in which the essential elements of the suggested hybrid system were omitted. The findings show erratic and imprecise stress identification when wavelet denoising and PCA fusion are excluded. A comparative study of image computation carried out on a single-board computer (SBC) versus in the cloud over a 5 G link demonstrated that the SBC processed data 8.27% faster than the cloud-based alternative over 5 G. The introduced approach enables more timely and accurate detection of water stress and offers substantial potential to boost crop output and curb water consumption in controlled-environment agriculture.

Keywords Remote sensing, IoT, 5G, Water stress, Plant canopy, Vegetation thermal analysis

*Correspondence:
Mikko Lahtinen
mikko.lahtinen@helsinki.fi
[1] Department of Artificial Intelligence for Barley and Oat Phenotyping, Faculty of Agriculture, University of Helsinki, Helsinki, Finland
[2] Department of Smart Greenhouse Climate Control Systems, Faculty of Agriculture, University of Eastern Finland, Kuopio, Finland
[3] Department of High-Throughput Phenotyping, Faculty of Agriculture, University of Turku, Turku, Finland

Introduction

IoT sensing devices find widespread application across the smart agriculture sector, greenhouses, and vertical farming operations. A variety of Industrial IoT (IIoT) sensors are employed to track greenhouse conditions, including air humidity and ambient temperature, as well as lighting control, such as UV LED growth lamps for photosynthesis. Likewise, certain IIoT sensors can be used for soil condition monitoring, including soil temperature and moisture content [1]. Soil moisture sensors come in two varieties: capacitive and resistive.

Furthermore, in recent years, the rapid evolution of remote sensing capabilities and the declining cost of hardware have led to the adoption of numerous camera types for plant remote monitoring in open fields [2] and, particularly, within

This is an open access article distributed under the terms of the Creative Commons Attribution-NonCommercial-ShareAlike 4.0 International License (CC BY-NC-SA 4.0), which permits non-commercial use, distribution, reproduction, and adaptation in any medium or format, provided that appropriate credit is given to the original author(s) and source, a link to the license is provided, and any changes made are indicated. Adapted material must be distributed under the same license.

© 2023 The Author(s). | Published by Agro Intelligence Research Press

greenhouses [3]. These imaging devices can be divided into three principal groups according to spectral sensitivity: visible light [4, 5], multispectral [6], and Thermal Infrared [7-10]. Each camera class can serve to classify observable leaf symptoms, assess chlorophyll levels or vegetation indices, and evaluate plant canopy temperature alongside stomatal conductance. Additional IoT tools used in greenhouses may include LiDAR to gauge plant architecture and growth velocity, or other instruments such as spot laser thermometers to record single-leaf temperature readings.

Prompt identification of water stress in lettuce is critical for the indoor cultivation sector, which carries substantial economic and environmental impacts. Efficient water stewardship in greenhouses is essential for optimizing yield and minimizing operational expenditures. Abiotic stresses, including water deficit in lettuce, can curtail yield with consequent financial impacts. In addition, early recognition of water stress supports precision irrigation of lettuce crops, enhancing sustainability by reducing waste. Our proposed method targets the demand in the greenhouse and vertical farming industries for water-efficient practices.

Water stress is an abiotic condition that can reduce plant productivity; conversely, irrigating without oversight or accuracy can subject plants to stress until the soil becomes excessively wet, potentially damaging the root system. Moreover, precision irrigation is crucial, particularly when aiming to cut water waste and achieve sustainability goals. Precision watering can be realized through IoT sensors and systems. Nonetheless, coupling remote sensing with these IoT instruments proves advantageous for accurately determining plant irrigation needs based on physiological indicators.

Notwithstanding progress in IoT sensor systems and remote imaging, many current methods for detecting water stress in indoor cultivation require updating. Conventional IoT sensors for tracking soil water content suffer from delayed stress identification. By comparison, remote sensing techniques that leverage thermal and visible-spectrum cameras can detect earlier physiological signs of water shortage.

Within smart agriculture, IoT—comprising interconnected sensor networks and devices—enables real-time observation and management. Edge computing enhances IoT by enabling data processing near the collection point, thereby reducing latency and improving the responsiveness of systems that require swift action, such as precision irrigation in greenhouses. Combining IoT with edge processing can aid smart farming by providing early, accurate water-stress warnings through real-time image analysis. This can positively affect more sustainable water utilization and bolster crop yields.

This paper introduces a new hybrid framework that unites Thermal Infrared (TIR) and RGB imaging through advanced picture processing methods—namely, wavelet denoising, Principal Component Analysis (PCA)-based fusion, and Gaussian Mixture Model (GMM) clustering—for the prompt and accurate recognition of water stress in lettuce. The suggested pipeline starts by extracting the plant canopy using HSV color-space background subtraction, an image-processing approach that refines the separation of green foliage from its background. Thermal image quality is improved through wavelet denoising, while PCA-based fusion of TIR and RGB data helps preserve detection accuracy regardless of structural shifts in the lettuce canopy. The approach then employs GMM to group stressed regions and applies false color to visually highlight affected zones. A comparative assessment was also undertaken to gauge the effect of removing wavelet denoising and PCA fusion. The data reveal markedly low accuracy if any vital module is omitted.

To validate the framework, an experiment comparing lettuce exposed to severe water deficit against regularly watered lettuce was executed. Soil moisture information was logged using IoT sensors, permitting a direct contrast between the proposed image-based method and conventional soil moisture readings. Additionally, all image analysis tasks were run both on a local IoT device using the suggested technique and in the cloud via a 5 G network. This design enabled a thorough comparison of processing time demands between local IoT execution and cloud computation, shedding light on performance efficiency and real-world feasibility.

The core objective of this research is to develop and validate an innovative method for early detection of water stress in lettuce using TIR and RGB imaging, coupled with advanced data processing. This method seeks to overcome the

© 2023 The Author(s). | Published by Agro Intelligence Research Press

shortcomings of current IoT sensors and remote sensing tools by enabling earlier and more reliable stress detection.

The principal contributions of this work include the creation of a novel hybrid framework that merges advanced image processing methods for isolating stress zones, effective grouping of plant canopy pixels via wavelet denoising, PCA-based fusion, and GMM clustering, a comparative analysis of the framework when crucial components are omitted, and a systematic approach for evaluating local versus cloud-based image computation. It further aims to offer a complete, accessible, and cost-efficient solution for water sustainability while simultaneously increasing crop yield.

The paper is organized as follows. Section 2 reviews related studies on water stress detection in open fields and greenhouses. Section 3 describes the materials and methods, covering the proposed technique, soil humidity data logging, image processing strategies, and computational time analysis between local IoT device processing and cloud execution. Section 4 reports the outcomes of the suggested hybrid framework alongside water-stress humidity thresholds, comparison findings when key modules are excluded, and processing time differences between local and edge-cloud image computation. In the 5 Discussion and 6 Conclusion, the discussion and its corresponding conclusions are presented.

Related Works

Scholarly publications contain numerous investigations into varied techniques for quantifying water stress across both field-based agriculture and controlled-environment cultivation. Open-field strategies include aerial remote sensing via Unmanned Aerial Vehicles (UAVs) or piloted aircraft, along with satellite observations exploiting specific spectral regions, such as the Shortwave Infrared (SWIR). Soil moisture probes and similar IoT devices find application in both outdoor fields and indoor growing facilities [1]. Meanwhile, inside controlled environments, practitioners deploy stationary, portable, or robot-mounted TIR or multispectral sensors to gather information reflecting crop hydration status.

Open field

Remote observation methods are a common tool in open-field contexts for evaluating vegetation hydration. High-definition pictures can be collected by UAVs, Unmanned Ground Vehicles (UGVs), and autonomous farming machinery. For more extensive survey areas, satellite platforms offer an alternative, albeit with reduced spatial detail.

Remote sensing

Gao *et al.* [11] describe a wide-ranging assessment of lettuce water content. The research team integrated data streams from reflectance spectroscopy, multispectral cameras, and canopy thermal readings. Their fused model delivers strong predictive power and consistency, outperforming single-sensor configurations in generalizability.

Chandel *et al.* [12] report a two-season study employing a specially engineered high-definition TIR and RGB acquisition setup for non-invasive tracking of hydration stress in winter wheat. The pipeline incorporated computer vision alongside deep learning classifiers; ResNet50 yielded the top classification result of 98.4% when fed TIR imagery, while a Deep Learning – Long Short-Term Memory (DL-LSTM) architecture reached 96.7%, the leading score within function-approximation models. These outcomes highlight the technique's suitability for accurate diagnosis and intervention of crop water stress.

While drones and satellite imagery provide reliable stress detection, their deployment requires a significant capital outlay and technical proficiency, posing hurdles for smaller-scale operations with tight budgets. By contrast, the hybrid framework proposed here, built on TIR and RGB imaging, provides a cost-effective and readily expandable approach to early water-stress identification in greenhouse settings.

Satellite imaging

© 2023 The Author(s). | Published by Agro Intelligence Research Press

Yao *et al.* [13] propose a technique that leverages SWIR reflectance products from the Moderate-resolution Imaging Spectroradiometer (MODIS) as surrogates for soil and plant water accessibility constraints within an adapted Priestley-Taylor formulation. Their results confirm the method's efficacy in deriving terrestrial latent heat flux (LE) and suggest its capacity to refine the representation of water constraints in regional LE modeling over China.

Moreno *et al.* [14] devised an operational procedure that blends meteorological inputs with MODIS-derived metrics—namely, the Normalized Difference Water Index (NDWI), the Shortwave Infrared Water Stress Index (SIWSI), and the Normalized Difference Index 7 (NDI7)—to reliably infer water stress in semi-natural plant communities reliably. This pipeline is a compelling alternative to classical meteorology-based approaches for characterizing year-to-year fluctuations in light-use efficiency (ε) across dryland and semi-dryland zones.

Indoor farming

The indoor cultivation sector regularly turns to remote sensing to infer leaf hydration and stomatal behavior. Image capture employs multispectral or TIR devices configured in fixed mounts, handheld formats, or robotic platforms.

Qiu *et al.* [15] propose a technique for disentangling the effects of insufficient water and elevated temperatures on species such as melon, tomato, and lettuce. Their method uses a reference dehydrated leaf, coupled with a transpiration transfer coefficient, to objectively measure environmental stress. The study confirmed strong separation between hydration-driven and heat-driven stress, establishing a linear association with a traditional CWSI baseline.

Grant *et al.* [16] examine the use of TIR imagery to infer stomatal aperture and leaf water condition. The work successfully separated watered from unwatered specimens across several plant types, producing strong correlations with porometry benchmarks. At the same time, it flagged difficulties stemming from leaf positioning and the consistency of 'wet' and 'dry' reference leaves in faithfully mirroring stomatal dynamics, supplying useful guidance for protocol design in crop management or ecological observation.

Ru *et al.* [17] formulate an improved irrigation management scheme for greenhouse-grown grapevines grounded in leaf temperature-derived CWSI. The outcomes confirm tight linkages to established plant water status parameters and reinforce the viability of this technology for tracking and modulating grapevine hydration stress.

Nuruddin *et al.* [18] examine how varying soil water deficit limits and irrigation timing regimes shape growth, output, and quality in greenhouse tomato crops. The study underscores that subjecting plants to water stress during the bloom stage yields better fruit yield and quality than stress imposed at other phenological phases or spread across the entire cultivation cycle.

Mangus *et al.* [19] put forward a fresh framework built around a TIR imaging system (TIRIS) to capture corn canopy temperature with high spatiotemporal granularity. The setup proves valuable for documenting spatial and temporal fluctuations in soil water content, thereby supporting scheduling and operational choices in precision irrigation management.

Established indoor farming approaches contribute usefully to recognizing plant water stress, but the technique introduced here offers unique strengths. Whereas prior work relies on either standalone remote sensing, narrowly defined environmental parameters, or conventional metrics such as CWSI, the proposed hybrid framework fuses Thermal Infrared (TIR) and RGB imagery with sophisticated analytical procedures to create a resilient, high-fidelity detection pipeline. The incorporation of HSV-based background extraction, wavelet-domain noise suppression, PCA-driven data integration, and GMM-based segmentation guarantees dependable stress localization. The method clusters thermal differentials and applies false-color labeling to stressed zones, enabling clearer visual interpretation for practitioners. Output accuracy empowers growers to intervene without delay. The system operates on affordable hardware, such as IoT processing units, thereby confirming its real-world feasibility. This design lowers economic obstacles to uptake while supporting scalability and broadening accessibility, even under resource-constrained conditions. Moreover, on-device image

© 2023 The Author(s). | Published by Agro Intelligence Research Press

computation enables efficient, accessible real-time analysis with limited reliance on external infrastructure. Ultimately, the proposed approach represents a cost-conscious solution for pinpointing water stress in lettuce crops, thereby improving production outcomes.

Materials and Methods

Two lettuce specimens served as the basis for the experiment. For tracking soil moisture trends, a pair of capacitive sensors was connected to a Raspberry Pi 3 Model B+ via an Arduino UNO, with readings captured at 1-hour intervals. A FLIR C5 camera (Teledyne FLIR LLC., USA) collected synchronized radiometric TIR and standard RGB imagery. To benchmark computational speed, the Raspberry Pi 3 Model B+ handled initial processing, after which a 5G modem transmitted data to a remote cloud server for the second phase of timing trials. The core objective of the proposed pipeline was to extract lettuce canopy and flag leaf pixels that display thermal indicators of stress based on relative temperature patterns within the TIR frame.

Experimental design

The study employed a pair of lettuce specimens (*Lactuca sativa* var. *capitata* L.) observed throughout a six-day window under laboratory conditions. One plant followed a standard watering schedule designed to hold soil moisture at roughly 70%, while its counterpart was subjected to acute water deprivation. Ambient parameters were held constant throughout the trial: air temperature was fixed at 17 °C and relative humidity (RH) at 60%. Photosynthetic lighting relied exclusively on artificial LED growth fixtures spanning wavelengths from 400 nm to 840 nm, mimicking the solar spectrum. The primary spectral contributions originated from blue light centered at 465 nm and red light centered at 625 nm, providing the most photosynthetically active wavebands for a 14-hour daily photoperiod.

The experimental run was conducted during the opening months of 2024 inside a sealed, environmentally regulated laboratory chamber, permitting uninterrupted measurement acquisition while safeguarding the imaging workflow against external perturbations—including environmental fluctuations—that might otherwise skew the findings.

In concrete terms, the laboratory implemented an atmospheric management system to stabilize both thermal and hygrometric conditions throughout the six days. Exterior illumination was entirely excluded, and the custom LED arrays served as the exclusive photon source to emulate natural daylight. Lettuce containers were arranged in a standardized geometric layout to guarantee uniform radiative exposure.

Soil moisture measure

Soil moisture sensors

A capacitive-type substrate moisture detector was embedded in the growing medium of each container, enabling synchronized acquisition of hydration readings. Capacitive detectors were preferred over their resistive counterparts due to a well-documented drawback of the latter: the passage of direct electrical current induces progressive corrosion at the electrode surfaces through electrolytic action, compounding the inherent degradation from prolonged soil contact. Structurally, a capacitive probe consists of three functional regions: an anode plate, a cathode plate, and the interstitial space separating them, which serves as the dielectric layer. Fundamentally, most capacitor designs incorporate a minimum of two conductive elements—commonly metallic sheets or films—partitioned by an insulating dielectric. Operationally, these devices respond to ionic species dissolved in the soil solution rather than directly measuring water volume.

Soil moisture sensors calibration

An Arduino Uno board was utilized to perform the calibration routine for the capacitive detectors. A dedicated script captured each unit’s output first in an air-dry environment and subsequently under full submersion in water, thereby

© 2023 The Author(s). | Published by Agro Intelligence Research Press

establishing the saturation ceiling and desiccation floor, respectively. These boundary measurements became the fixed calibration offsets applied to each sensor for all subsequent experimental readings.

The calibration protocol unfolded in two successive phases. The initial step involved situating every detector in a moisture-free medium and recording its baseline electrical response. The second step required immersing the probes in liquid water to document the signal level corresponding to complete saturation. The captured values were then transformed into sensor-specific calibration constants. A confirmatory procedure was followed, in which detector outputs were benchmarked against growth media prepared at known moisture levels to validate the reliability of measurements collected during the actual experiment.

Logging soil moisture data

Given that the capacitive probes generate analog voltage signals, the data logging sequence commenced with the Arduino UNO polling each detector at one-hour intervals, scaling the raw readings according to the previously determined calibration constants. This microcontroller was interfaced with a Raspberry Pi 3 Model B+ single-board computer, where a Python script appended a new row to a comma-separated values (CSV) file every hour, recording the timestamp and the percentage moisture value for each probe. The hardware interconnection scheme is depicted in **Figure 1**.

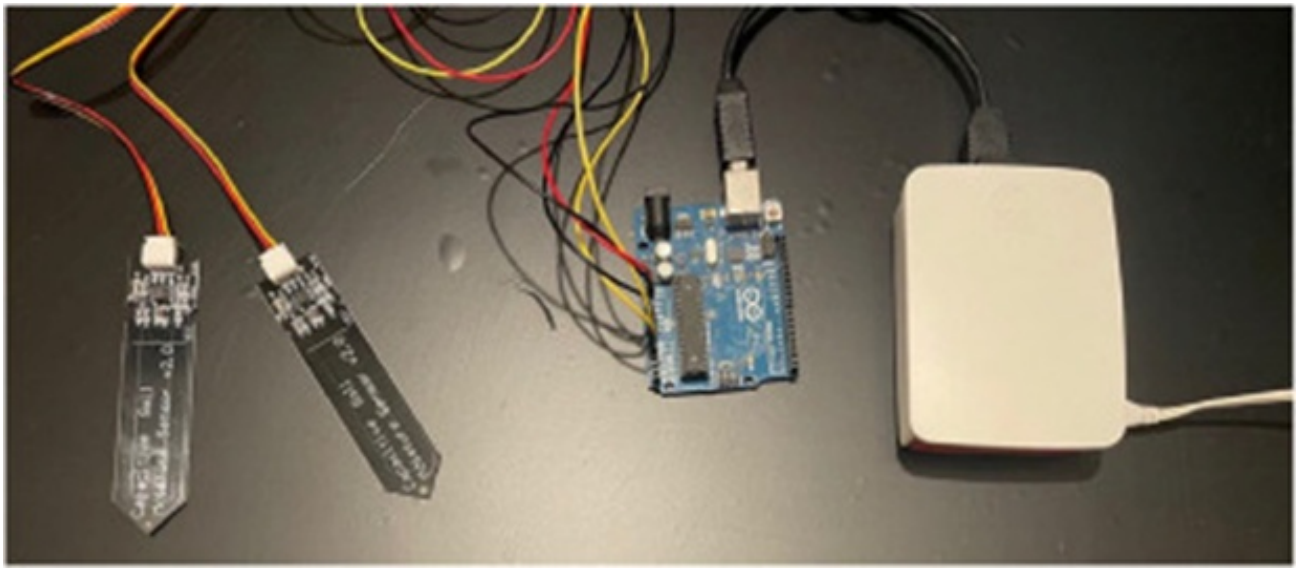

Figure 1. The connection of Raspberry Pi 3 Model B+, Arduino UNO, and Capacitive Soil Moisture Sensor.

Remote sensing

A FLIR C5 unit, housing both TIR and RGB detector arrays, served as the imaging instrument, capturing photographs of each lettuce specimen at roughly 12-hour intervals. Over the entire experimental duration, 26 thermal frames, each containing a co-registered RGB image, were collected. The FLIR C5 device simultaneously acquires radiometric thermal data and visible-light imagery, embedding RGB information and metadata within the thermal file container. Its thermal sensor operates within the 8–14 μm wavelength band. **Table 1** enumerates the detailed technical parameters of the TIR and RGB imaging channels, specifying focal length, spatial resolution, radiometric bit depth, megapixel rating, angular field of view, and file compression scheme.

Table 1. TIR and RGB specifications.

Specifications	RGB	TIR

© 2023 The Author(s). | Published by Agro Intelligence Research Press

Focal length	1.54 mm	1.9mm
Resolution	640 × 480	160 × 120
Bit depth	8	8
Megapixels	5.0	0.307
Field of view	71.5 deg	53.6 deg
Compression	JPEG	JPEG

Hybrid image processing framework

The novel hybrid image analytics pipeline weaves together multiple sophisticated computational methods—wavelet-domain noise attenuation, PCA-mediated data integration, and GMM-based segmentation—to sharpen water stress discrimination. Although isolated elements of this toolkit have appeared in earlier publications, their deliberate orchestration within a unified processing chain yields a detection mechanism with superior resilience and fidelity. The supplementary computation of stressed-area proportions and the graphical annotation of affected zones through false-color rendering further translate the outputs into actionable intelligence, distinguishing this workflow from established methodologies [20].

Background isolation

The visible-light RGB frame provides the basis for delineating the lettuce canopy from its backdrop. The color image is converted to the HSV color space, after which a set of threshold criteria—Hue channel values exceeding 60 but remaining below 85, Saturation channel values under 50, and Value channel readings above 150—are used to construct a binary mask that suppresses non-canopy regions. A representative outcome is shown in **Figure 2**. This preprocessing stage is vital for attenuating extraneous signal contributions and facilitating the reliable demarcation of stressed tissue.

© 2023 The Author(s). | Published by Agro Intelligence Research Press



Figure 2. Background isolation of the RGB image using the HSV model.

Wavelet denoising

Thermal infrared captures are frequently contaminated by stochastic fluctuations that can smear the subtle temperature differentials symptomatic of plant water deficit. The application of wavelet-based denoising attenuates such interference while safeguarding diagnostically relevant detail, particularly the thermal patterns indispensable for downstream interpretation, as shown in **Figure 3**. This enhancement step yields crisper TIR frames and, correspondingly, elevates the reliability of subsequent stress classification [21].

© 2023 The Author(s). | Published by Agro Intelligence Research Press



Figure 3. Wavelet Denoising of the TIR image.

RGB-TIR image fusion

The integration of visible-band and thermal imagery amalgamates complementary streams of information spanning the reflective and emissive domains, thereby supporting a more holistic evaluation of vegetation health. PCA accomplishes this synthesis by compressing the feature space and prioritizing the most information-rich components. The resultant composite frame accentuates stress signatures that might elude detection when either modality is inspected in isolation, reinforcing the capacity to flag stress-induced physiological anomalies [22]. **Figure 4** offers an illustrative example of PCA-mediated RGB-TIR fusion.

© 2023 The Author(s). | Published by Agro Intelligence Research Press

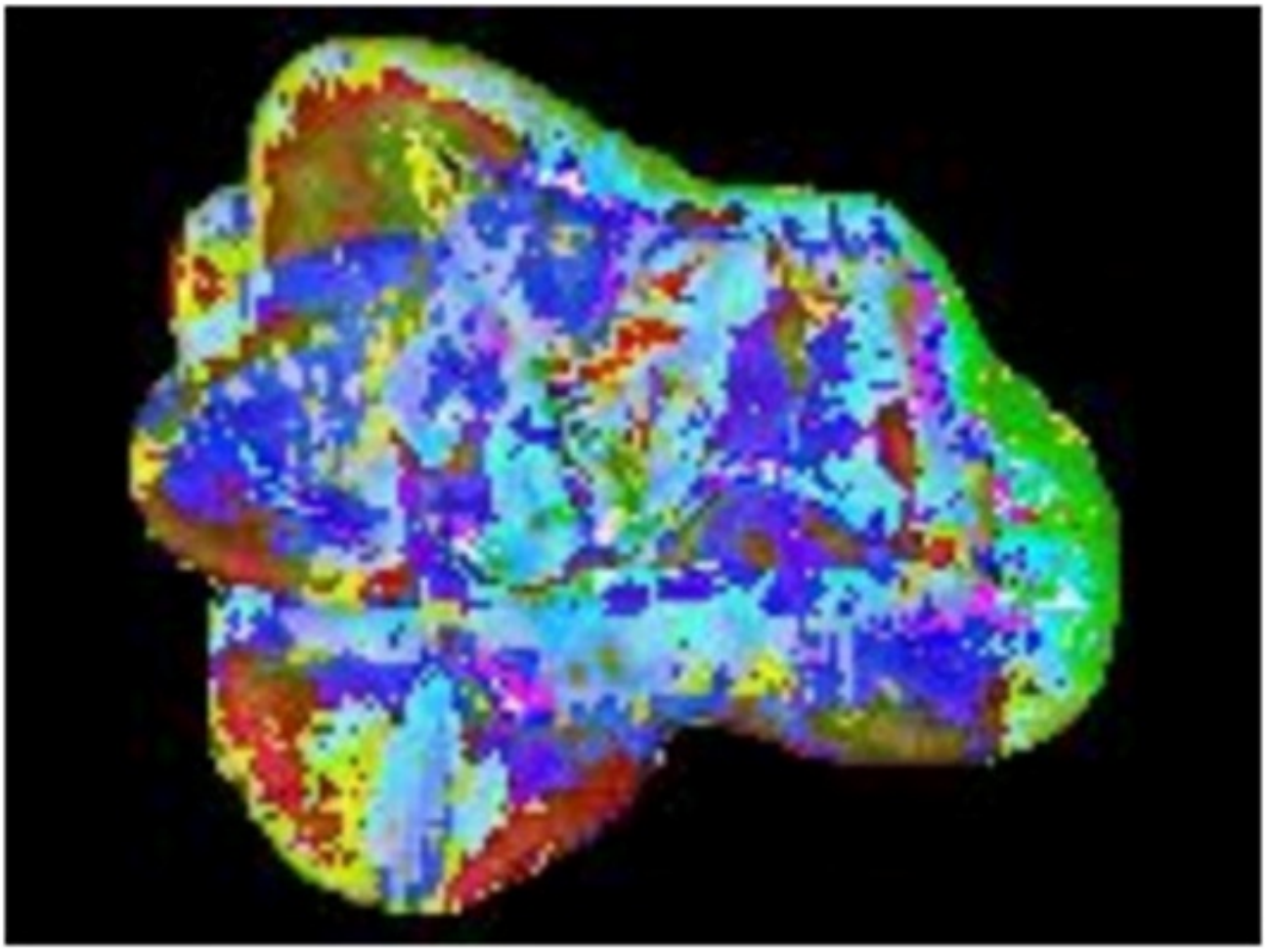

Figure 4. Fused Image of the TIR and RGB image using PCA.

Gaussian mixture model (GMM) clustering

Canopy-associated pixels in the fused image are partitioned using a GMM, which subdivides the scene into coherent groupings based on the statistical distribution of intensity values. By conceptualizing the pixel population as a weighted combination of multiple Gaussian density functions, the GMM framework proves adept at isolating clusters reflective of graduated stress intensities. This probabilistic formulation enables the categorical separation of stressed versus non-stressed canopy sectors [23]. The silhouette coefficient criterion was computed across the ensemble of fused-image canopy pixels to ascertain the optimal number of partitions (k). The analysis indicated that six clusters constituted the most parsimonious yet descriptive representation; accordingly, canopy pixel values from all fused images were allocated among six groupings, as exemplified in **Figure 5**.

© 2023 The Author(s). | Published by Agro Intelligence Research Press

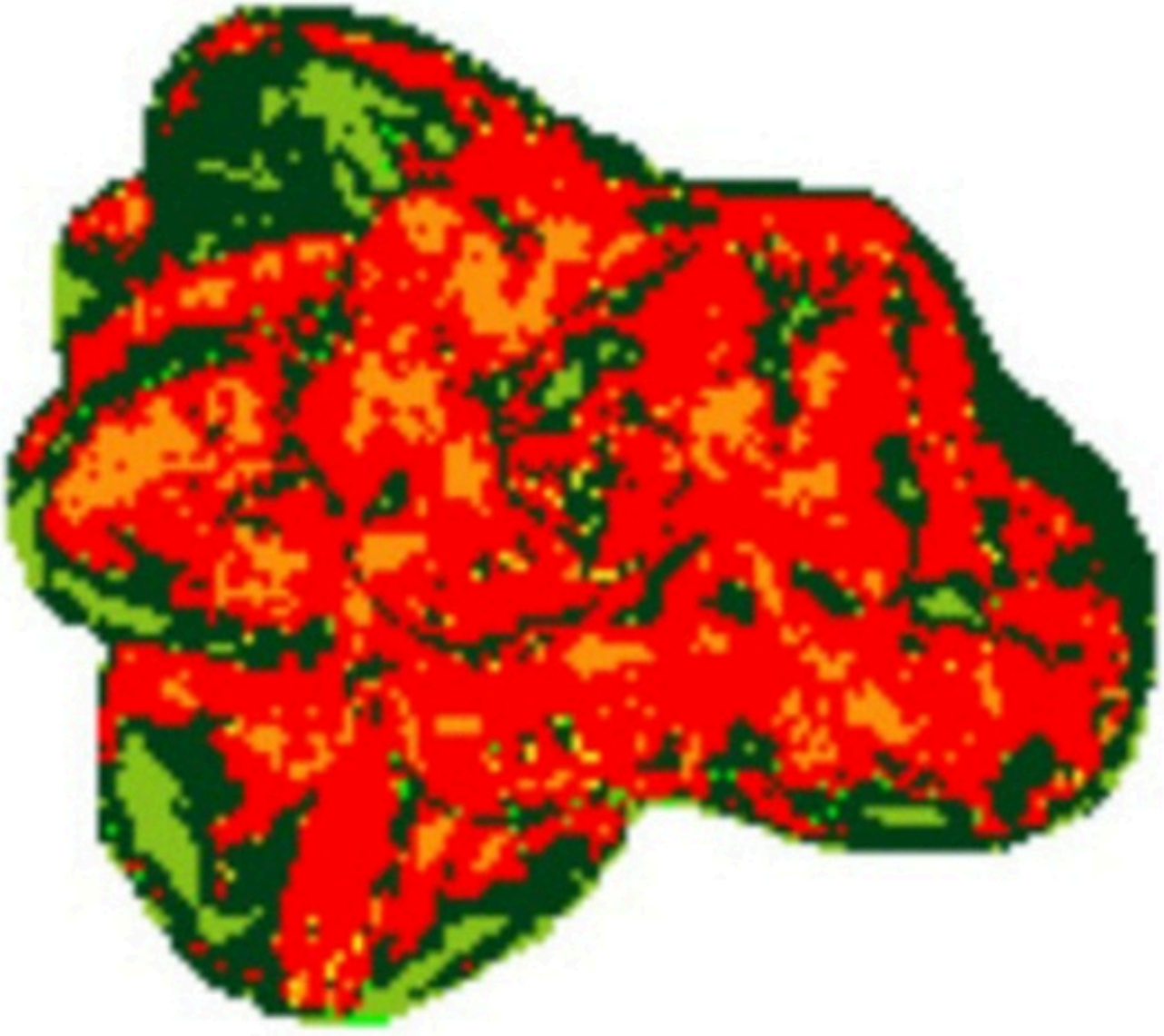

Figure 5. Clustering of the Fused image using GMM.

Pseudo-coloring of stress

For each acquisition time point, the two uppermost clusters—those associated with the highest thermal signatures and therefore representing the tissue most severely impacted by stomatal closure—were singled out. The spatially corresponding pixels within the RGB image were then highlighted using a yellow false-color overlay, as demonstrated in **Figure 6**.

© 2023 The Author(s). | Published by Agro Intelligence Research Press

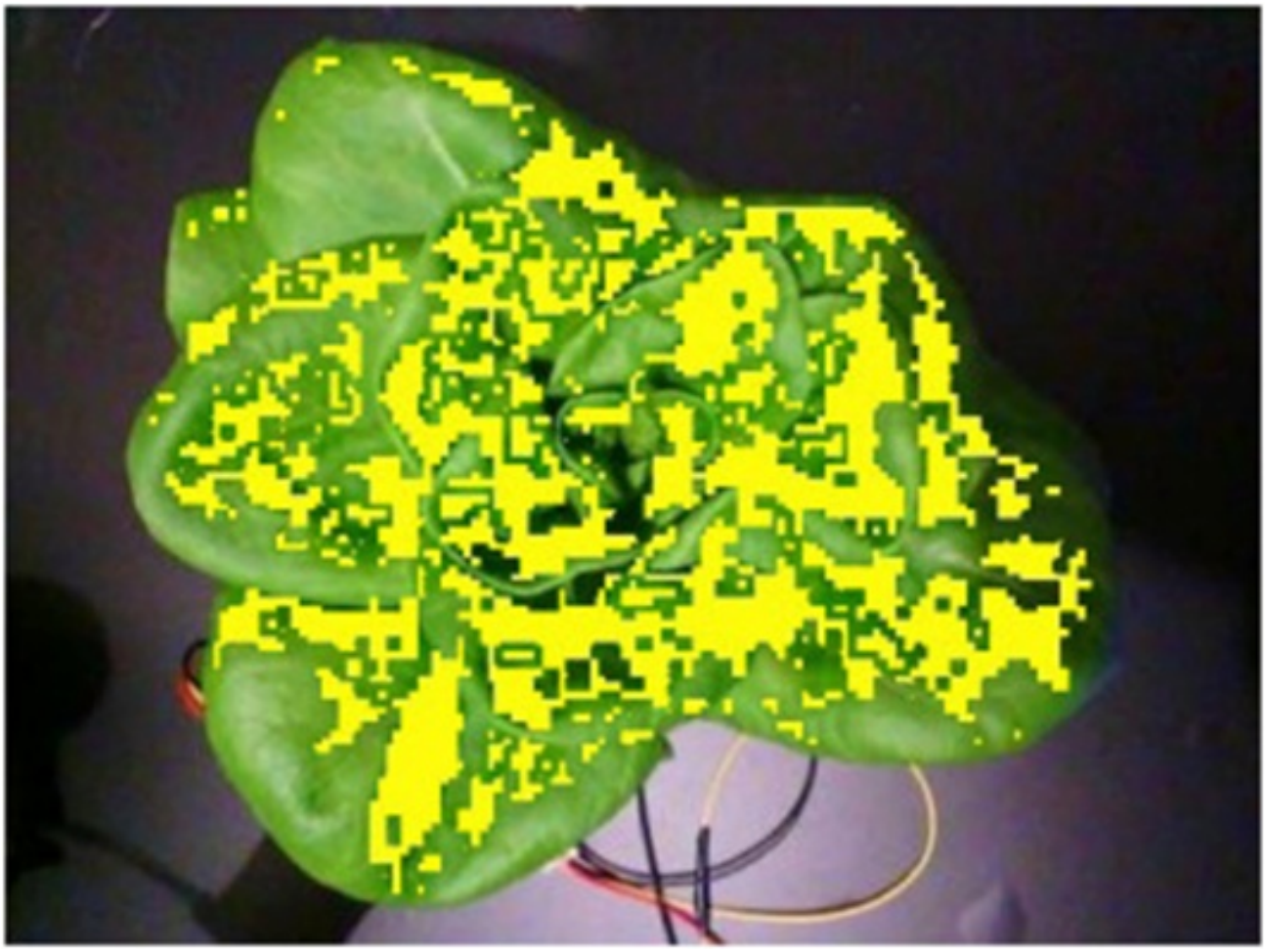

Figure 6. Stressed area pseudo-coloring.

Framework flowchart

A schematic diagram delineates three processing trajectories that collectively map the architecture of the proposed hybrid pipeline and its comparative evaluation schema. The primary trajectory corresponds to the unabridged hybrid framework, encompassing its entire suite of modules: wavelet denoising, PCA-driven RGB-TIR fusion, and GMM clustering. This trajectory serves as the gold standard for evaluating the methodology's performance.

The secondary and tertiary trajectories portray versions of the framework from which pivotal modules have been excised to probe their individual contributions. The second trajectory strips out both wavelet denoising and PCA-based fusion, compelling the pipeline to operate directly on unprocessed thermal imagery—bereft of noise mitigation and without harnessing the complementary visible-spectrum channel. This variant investigates the extent to which measurement noise and the forfeiture of RGB information degrade the precision of stress detection and the coherence of clustering outputs. The third trajectory eliminates only the PCA-mediated fusion step, processing the thermal and RGB data as parallel, independent streams rather than as an integrated whole. This configuration scrutinizes the importance of blending emissive and reflective data, especially under conditions where canopy geometry modulates stress manifestation. The flowchart reproduced in **Figure 7** maps the sequence of data transformations traversing these three trajectories.

© 2023 The Author(s). | Published by Agro Intelligence Research Press

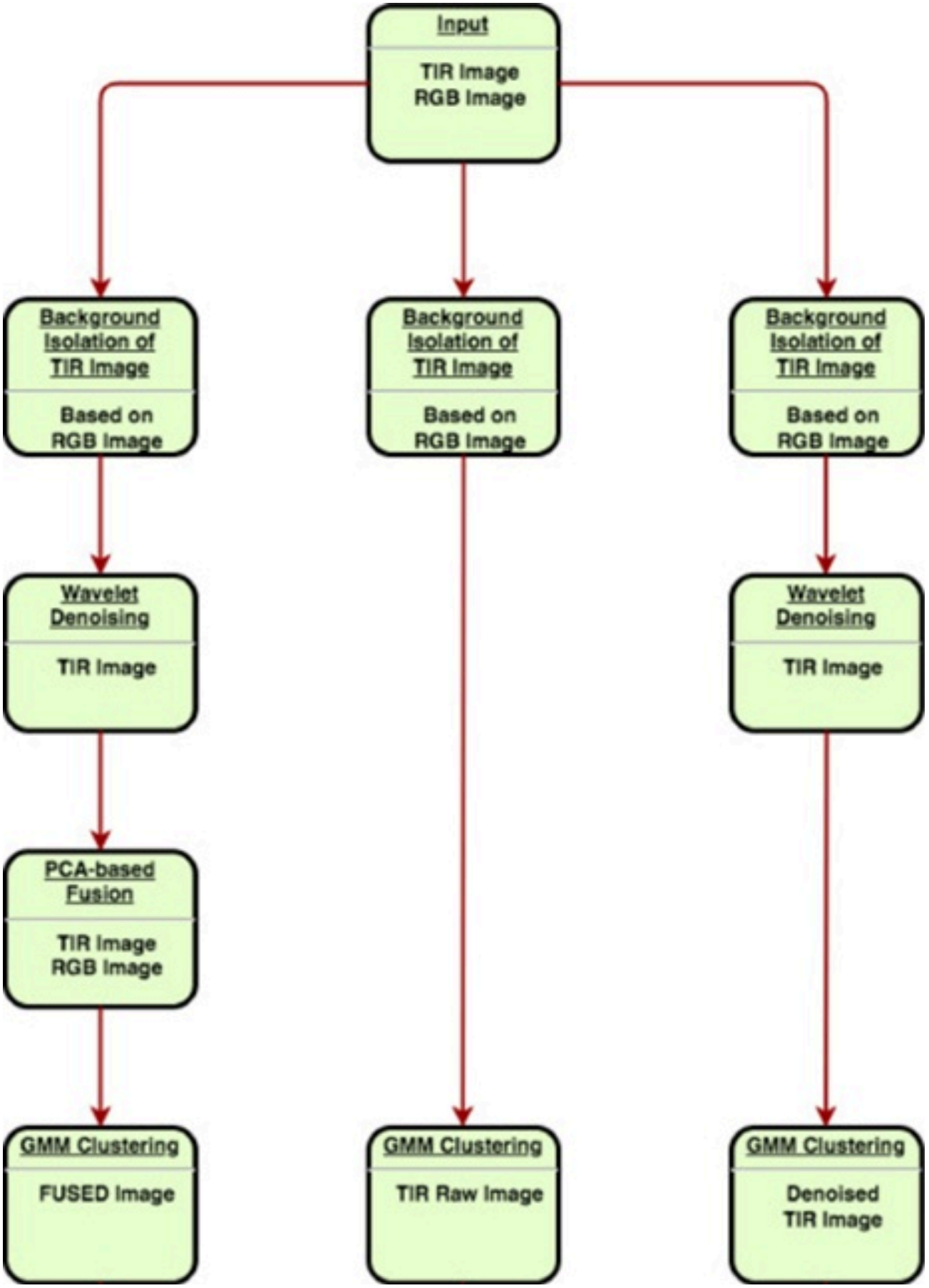

© 2023 The Author(s). | Published by Agro Intelligence Research Press



© 2023 The Author(s). | Published by Agro Intelligence Research Press

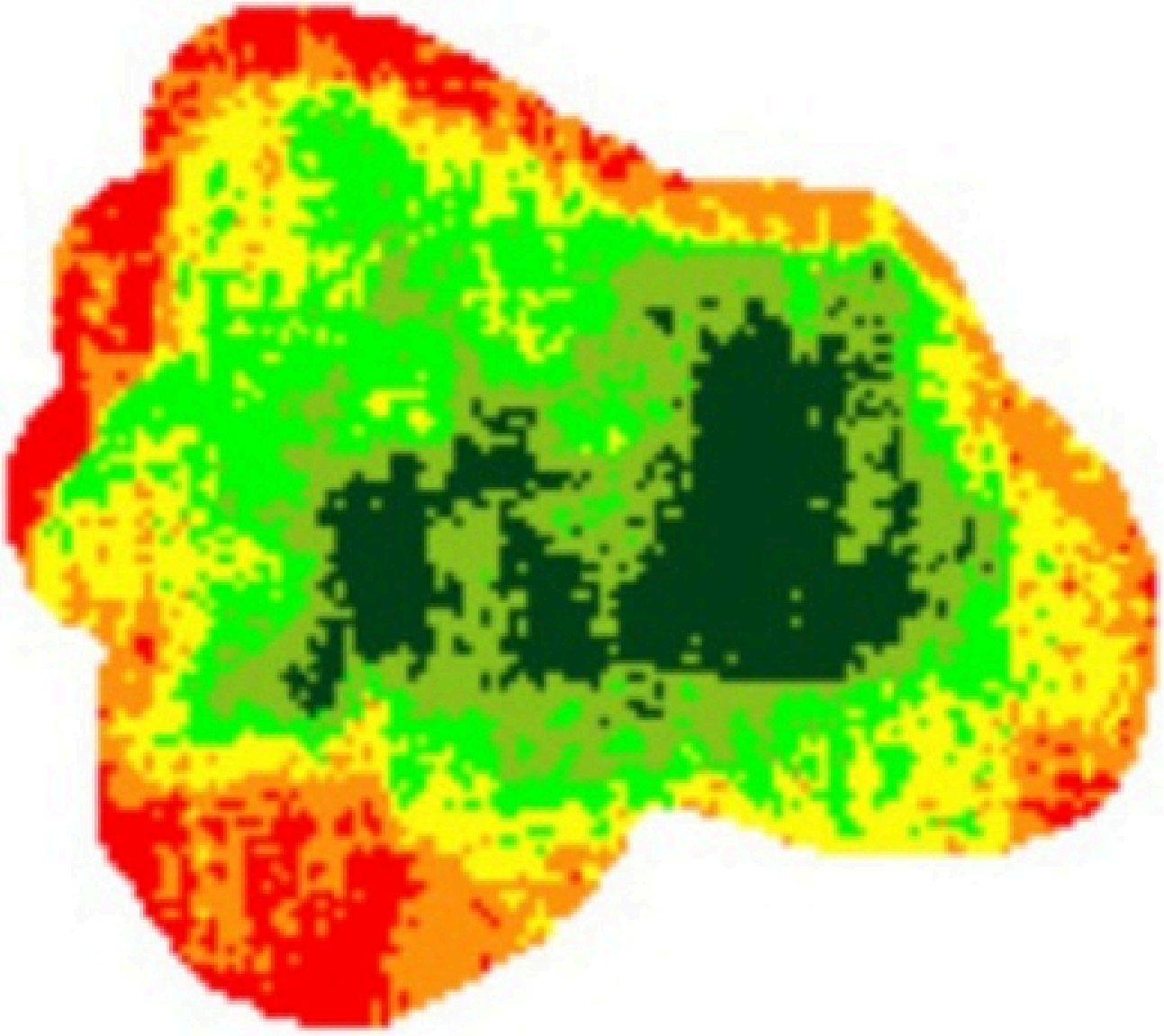

(a)

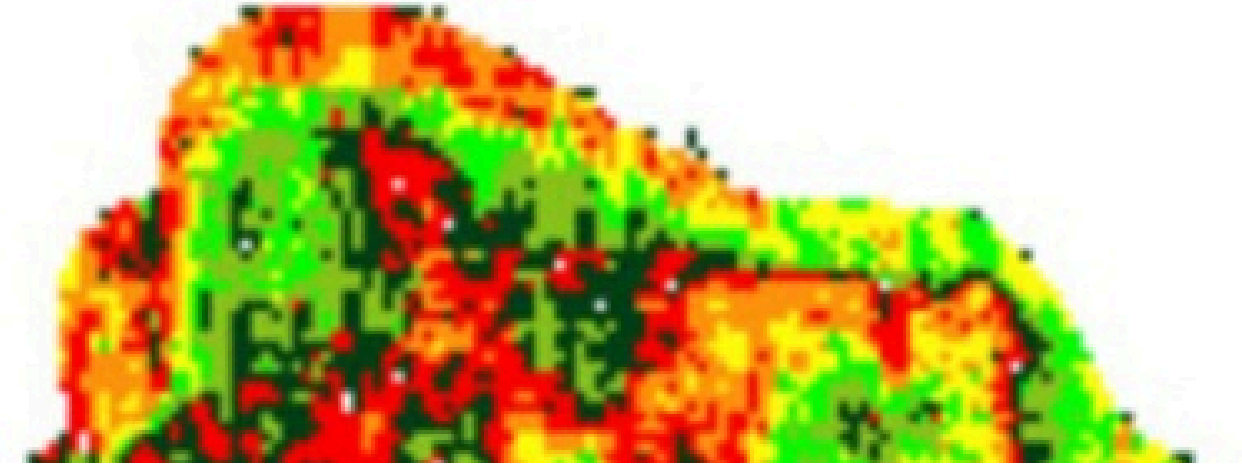

© 2023 The Author(s). | Published by Agro Intelligence Research Press

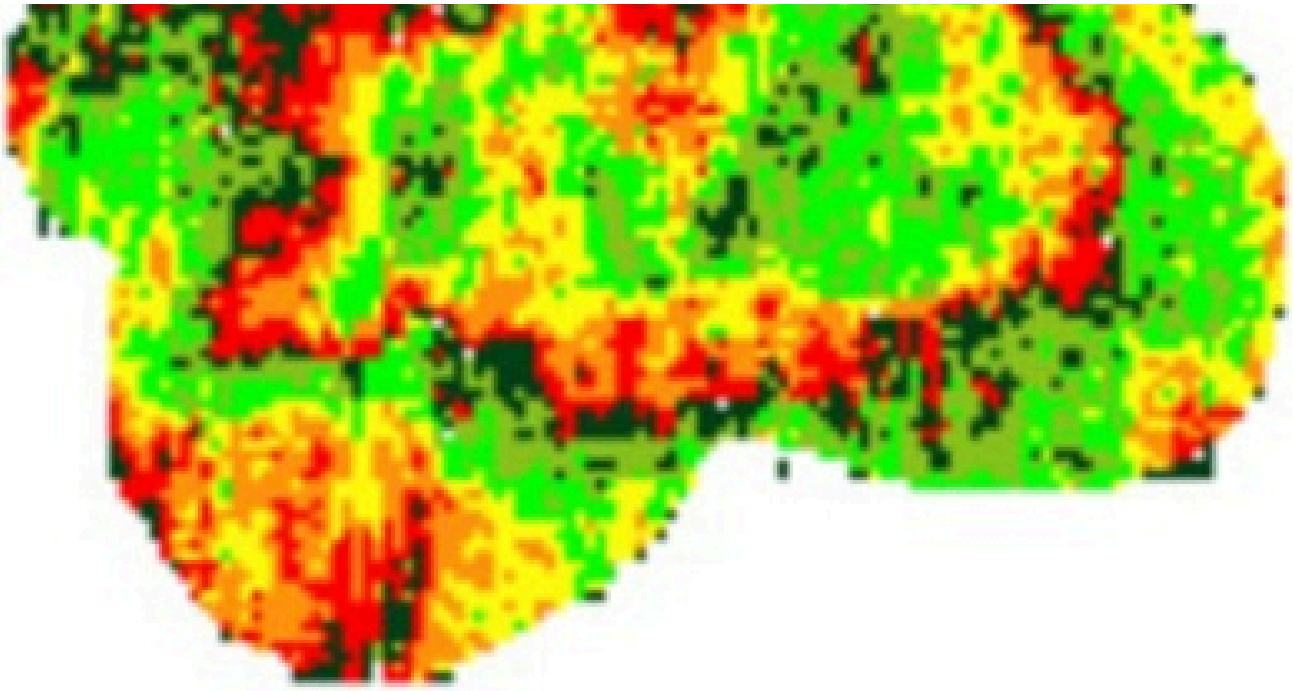

(b)

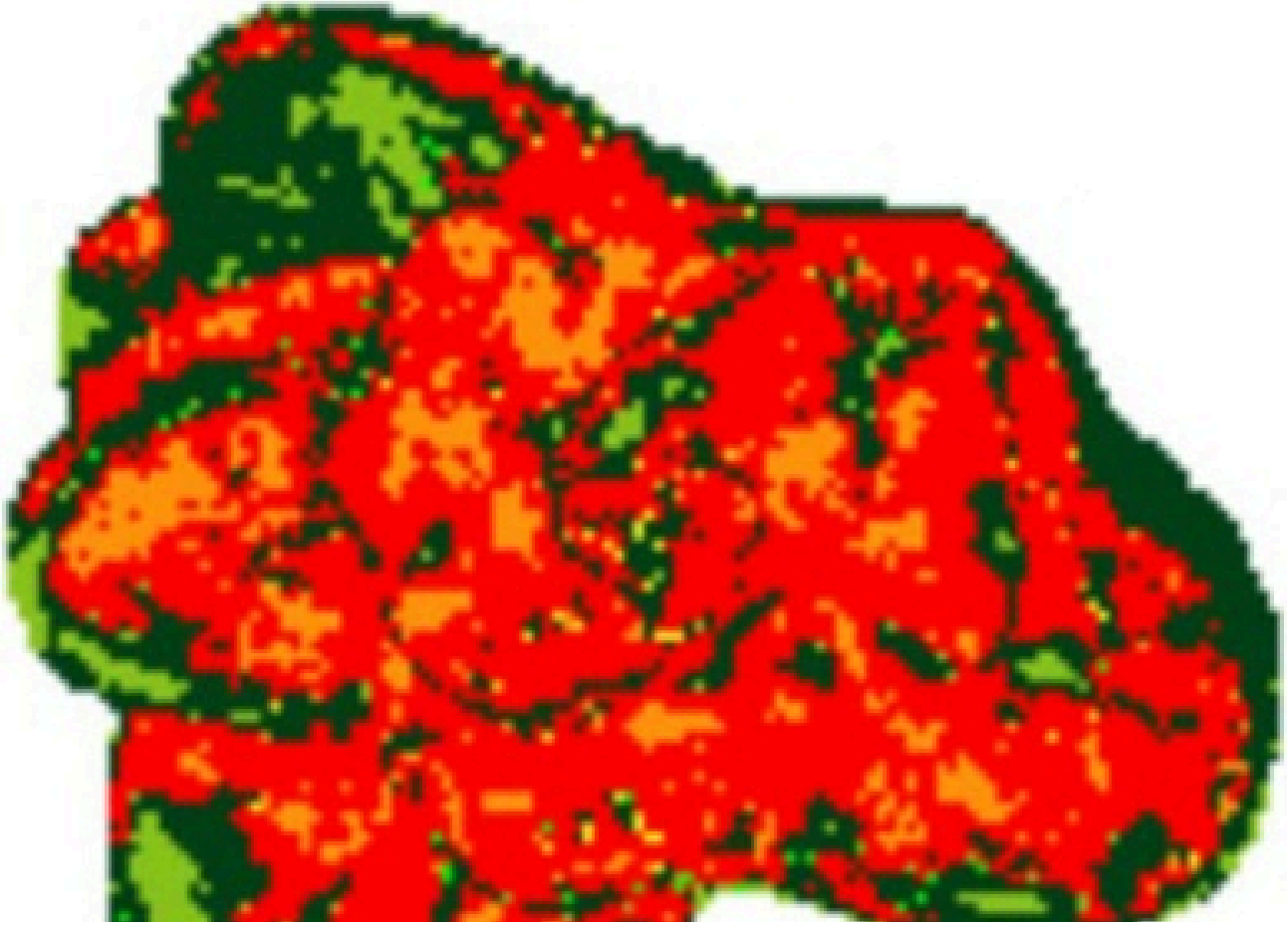

© 2023 The Author(s). | Published by Agro Intelligence Research Press

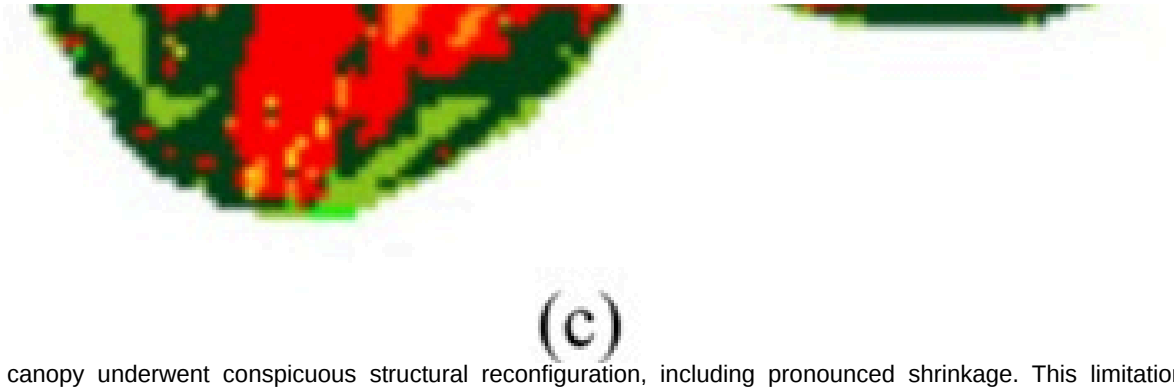

(c)

lettuce canopy underwent conspicuous structural reconfiguration, including pronounced shrinkage. This limitation is plainly visible in **Figure 9**, which juxtaposes the canopy morphologies of the stressed and regularly watered specimens at the trial's final stage.

© 2023 The Author(s). | Published by Agro Intelligence Research Press



(a)



© 2023 The Author(s). | Published by Agro Intelligence Research Press



(b)

Stress percentage measurement

The full complement of pixels making up the lettuce canopy in the RGB-derived masked image, together with the count of yellow-highlighted pixels in the pseudo-colored rendition denoting stressed tissue as identified by the hybrid processing workflow, were enumerated to determine the stress percentage attributable to each lettuce plant in every captured frame, as collated in **Table 2**. The stress percentage was obtained by dividing the stressed pseudo-colored pixel tally by the overall canopy pixel total, as formulated in **Eq. 1**. In addition, to corroborate the proposed technique's findings, a manual visual survey was conducted to document outward manifestations of leaf stress in lettuce subjected to extreme water shortage at each successive stage of the experiment. A comparative visual display of symptomatic features, including canopy extent and structural divergence, for the control and drought-stressed plants after the 96-hour mark is shown in **Figure 9**.

$$SP = \frac{S}{L} \quad (1)$$

Table 2. Stress percentage per 12 h.

Time (Hours)	Stress percentage	
	Stressed lettuce	Normal lettuce
0	19.2%	0.6%
12	30%	1.2%
24	41.2%	0.5%
36	40.2%	1.3%
48	42.3%	0.2%
60	43.05%	0.9%
72	41.3%	0.3%
84	44.1%	0.7%
96	46.02%	0.3%
108	45.1%	0.2%
120	47.4%	0.4%
132	43.3%	1.1%
144	48.1%	1.3%

© 2023 The Author(s). | Published by Agro Intelligence Research Press

The total pixel population of the lettuce canopy within the RGB-masked image (L) and the stressed pixel population within the pseudo-colored image (S) were tallied to compute the stress percentage (SP) for each lettuce specimen at every temporal sampling point.

Statistical analysis

The efficacy of the proposed hybrid framework for detecting water stress in lettuce crops was evaluated through statistical comparisons with capacitive soil moisture sensors. A paired t-test was selected as the analytical instrument, deployed with the specific aim of determining whether the observed performance differential between the proposed methodology and dependence on soil moisture probes for water stress identification reached the threshold of statistical significance.

Arithmetic means and standard deviations were derived as part of the statistical assessment, complementing the paired t-test procedure. The mean (average) encapsulates the central tendency of water stress detection accuracy and is computed as outlined in **Eq. 2**.

$$Mean = \frac{\sum x_i}{N} \quad (2)$$

Where:

• xi represents the individual water-stress detection values logged at each successive time interval.

• N signifies the total number of measurement instances, which in the context of this study equaled 13 temporal intervals.

The mean water-stress detection accuracy of the Proposed Hybrid Framework was calculated as shown below.

$$Mean\ (Proposed\ Method) = \frac{19.2+30.0+41.2+...+48.1}{13} = 42.98\%$$

In parallel, the mean accuracy attributable to Soil Moisture Sensors was determined at 55.54%. These mean values supply a preliminary comparative snapshot, conveying the typical performance level of each technique over the experiment's full time course. Standard deviation (SD) was calculated using **Eq. 3** to assess the consistency of water stress detection accuracy. The SD captures how widely individual data points scatter away from the mean, offering a gauge of each method's dependability.

$$SD = \sqrt{\frac{\sum (x_i - \mu)^2}{N-1}} \quad (3)$$

Where:

• xi denotes the individual stress detection readings.

• μ represents the mean stress detection accuracy.

• N corresponds to the total measurement count (13 time intervals).

© 2023 The Author(s). | Published by Agro Intelligence Research Press

Reliance on soil moisture sensors for water stress detection results in broader fluctuations and a greater likelihood of inconsistency, as evidenced by a standard deviation of 23.46%. On the other hand, the standard deviation associated with the proposed method, at 7.80%, indicates a notably tight clustering of results and thus high consistency in water stress identification.

A paired t-test was run to determine whether the performance disparity between the two water-stress detection strategies was statistically significant. The paired t-test is a statistical technique for comparing two interrelated sample groups. The mean difference ($\bar{d}$) was used to express the average magnitude of the performance gap. In contrast, the standard deviation of the differences (sd) quantified the extent of fluctuation in water-stress detection accuracy across the two modalities. The t-statistic (t) was obtained as specified in **Eq. 4**.

$$t = \frac{\bar{d}}{s_d/\sqrt{n}} = \frac{-12.56}{1.34/\sqrt{13}} = -9.40 \quad (4)$$

The negative t-statistic indicates an inverse temporal relationship between the two techniques. The proposed method detected elevated water-stress percentages at early time points, whereas the soil moisture sensors only indicated water stress after substrate moisture content had dropped substantially. This temporal offset confirms that the proposed technique furnishes both earlier warning and more faithful water stress detection.

The degrees of freedom (df) were derived following **Eq. 5**.

$$df = N - 1 = 13 - 1 = 12 \quad (5)$$

Drawing on the t-statistic magnitude together with 12 degrees of freedom, the corresponding p-value was established to be $P < 0.001$. A p-value of this order indicates a highly significant divergence between the two approaches, underscoring that the proposed methodology detects water stress at a considerably earlier stage, thereby enabling more prompt intervention and more efficient water resource stewardship.

Computational time cost

The entire batch of captured images was fed into a Python routine that leveraged multiprocessing in accordance with the proposed hybrid image analysis workflow. Execution took place first on a local IoT platform—a Raspberry Pi 3 Model B+ sporting a quad-core 1.2 GHz processor and 1 GB of memory, combining for 4.8 GHz of total computational throughput—and subsequently on a remote cloud setup reached through a 5 G connection, so that processing durations could be directly contrasted. On the IoT device, the image collection took 209.85 s. For the edge-cloud pathway, the clock was split across two sequential stages: the first segment measured the time the image batch spent traveling to the cloud virtual instance, and the second measured the actual computation time on that remote machine. Each frame was sent to the cloud instance via a 5G adapter mated to the Raspberry Pi 3 Model B+, achieving a steady upload rate of 45.7 Mbps. The cloud side operated with a pair of virtual CPUs, each clocking a base frequency of 2.25 GHz, backed by 4 GB of memory—an arrangement delivering 4.5 GHz of aggregate processing muscle. Total wall-clock time reached 228.79 s, carved into 26.37 s consumed by data transmission and 202.42 s spent on number crunching. **Table 3** itemizes the elapsed times per method and breaks out the edge-cloud figures into the upload fraction and the computation fraction.

Table 3. Processing time.

Type of processing	Time (seconds)		
	Uploading	Computational	Total

© 2023 The Author(s). | Published by Agro Intelligence Research Press

IoT	–	209.85	209.85
Cloud	26.37	202.42	228.79

Results and Discussion

The hybrid image processing framework proposed in this study reliably flags water stress in lettuce at an early stage. The pipeline harnesses wavelet denoising, PCA-driven RGB-TIR fusion, and GMM clustering. It substantially outperforms soil moisture probes at detecting water stress in lettuce specimens. This portion of the paper unpacks the hybrid framework's operational results and examines the accuracy penalty incurred when essential building blocks—specifically wavelet denoising and PCA fusion—are removed. A runtime comparison of the proposed framework running locally versus on cloud resources is likewise supplied.

Performance of the full hybrid framework

The full hybrid framework generated outputs characterized by early water-stress recognition and strong detection accuracy. The interplay among wavelet denoising, PCA-mediated RGB-TIR fusion, and GMM clustering enables stress discrimination at the individual-pixel level. One of the standout findings was the ability to signal water stress in lettuce up to 84 h before a soil moisture sensor's alert. Stress percentages derived through the proposed technique, plotted alongside soil moisture trajectories for both the adequately watered and the drought-subjected lettuce at 12-hour increments beginning from hour zero, appear in **Table 4** and **Figure 10**. Equally important, the stress percentage figures inferred from pseudo-colored stress zones remained stable through all measurement windows, even as the canopy geometry of the unwatered lettuce shifted in response to the physiological strain of dehydration. This resilience can be attributed to the way RGB-TIR fusion successfully tracks the structural evolution of the lettuce canopy across all experimental stages.

Table 4. Stress and soil moisture percentage per 12 h.

Time (hours)	Soil humidity		Stress percentage	
	Stressed lettuce	Normal lettuce	Stressed lettuce	Normal lettuce
0	75%	75%	19.2%	0.6%
12	75%	74%	30%	1.2%
24	76%	76%	41.2%	0.5%
36	74%	75%	40.2%	1.3%
48	73%	73%	42.3%	0.2%
60	71%	76%	43.05%	0.9%
72	69%	74%	41.3%	0.3%
84	64%	76%	44.1%	0.7%
96	58%	76%	46.02%	0.3%
108	46%	75%	45.1%	0.2%
120	31%	74%	47.4%	0.4%
132	20%	73%	43.3%	1.1%

© 2023 The Author(s). | Published by Agro Intelligence Research Press

144	8%	73%	48.1%	1.3%

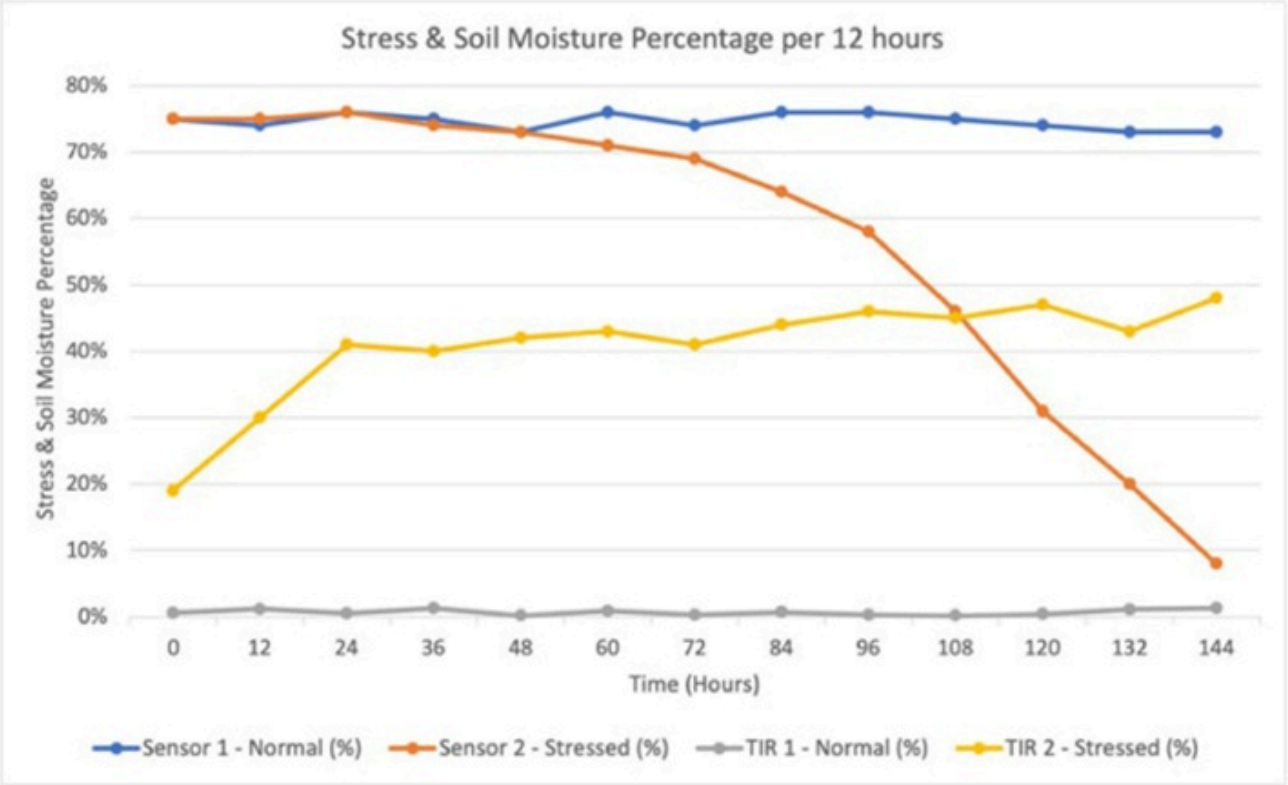

Figure 10. Comparison of stress and soil moisture percentage.

Statistical testing confirms that the proposed approach yields more accurate water stress detection than soil moisture sensors. Specifically, the paired t-test yields a statistically significant result ($t = -9.40$, $df = 12$, $P < 0.001$), as shown in **Table 5**, indicating that the proposed method provides earlier warnings and greater precision in pinpointing water stress in lettuce.

Table 5. Comparison of stress detection accuracy using a paired t-test.

Method	P-value	Degrees of freedom	t-statistic	Standard deviation (%)	Mean (%)
Proposed hybrid framework	< 0.001	12	−9.40	7.80	42.98
Soil moisture sensors	N/A	N/A	N/A	23.46	55.54

Effect of excluding wavelet denoising and PCA fusion

Wavelet denoising plays a vital role in cleaning the noise floor of TIR frames. At the same time, PCA fusion is equally critical for integrating visible-band and thermal-band information, especially when the drought-stressed lettuce canopy undergoes physical reconfiguration. Both modules were removed from the pipeline to assess their impact on the overall scheme, with particular attention to the integrity of GMM clustering and the reliability of water stress detection. Dropping wavelet denoising leaves a substantial noise residue in the thermal images, which, in turn, degrades GMM cluster coherence and introduces volatility into water-stress estimates. Concurrently, doing without PCA fusion means the system can no longer compensate for canopy structural drift, leading to mislabeled stress regions and disjointed GMM clusters.

© 2023 The Author(s). | Published by Agro Intelligence Research Press

Detection outcomes under the variant that lacks both wavelet denoising and PCA fusion are riddled with inconsistency and error; tellingly, at the 24-hour mark, the stress percentage attributed to the normally watered lettuce balloons to 32.7%, versus a mere 0.5% under the intact hybrid framework. The erratic swings in stress percentage for both the irrigated control and the non-irrigated specimen are chronicled in **Table 6**. The twin handicaps of noise-corrupted thermal data and the missing RGB-TIR linkage—especially the consequent blindness to canopy restructuring—render the system incapable of cleanly partitioning stressed from unstressed tissue, let alone detecting water stress faithfully. These observations underscore that wavelet denoising and PCA fusion are foundational prerequisites for robust clustering and, above all, for trustworthy water-stress determination.

Table 6. Stress percentage per 12 h, omitting wavelet denoising and PCA fusion.

Time (hours)	Stress percentage	
	Stressed lettuce	Normal lettuce
0	17.3%	16.7%
12	19.3%	18.2%
24	31.6%	32.7%
36	21.5%	23.9%
48	10.9%	31.8%
60	17.3%	25.8%
72	26.6%	26.7%
84	24.6%	27.8%
96	34.2%	27.9%
108	27.04%	28.2%
120	24.03%	31.8%
132	20.5%	29.1%
144	18.2%	18.2%

Effect of excluding PCA fusion

PCA-mediated RGB-TIR fusion serves as a cornerstone for accurate water-stress identification, particularly when physiological adjustments reshape the canopy's form. Stress percentage readings logged when PCA fusion was switched off deviated from the accuracy target, with the largest departures occurring during the experiment's concluding phases, as shown in **Table 7**. Likewise, without PCA-driven fusion, the zones flagged as stressed during the GMM clustering step were delineated with much less consistency and sharpness than in the complete hybrid framework. The absence of PCA fusion carries severe consequences, especially when canopy architecture enters a state of flux, leading the system to classify stressed sectors erroneously. The canopy configuration—and especially the outer leaf arrangement—of the stressed lettuce underwent a dramatic transformation between the initial 12-hour snapshot and the 144-hour observation point under relentless water withholding, a divergence captured in **Figure 9**. These results confirm that retaining PCA fusion is non-negotiable for safeguarding the framework's accuracy and for achieving precise stress localization, in particular when the lettuce canopy experiences physical deformation.

Table 7. Stress percentage per 12 h, omitting PCA fusion.

© 2023 The Author(s). | Published by Agro Intelligence Research Press

Time (Hours)	Stress percentage	
	Stressed lettuce	Normal lettuce
0	7.3%	8.2%
12	10.01%	12.1%
24	12.1%	12.2%
36	12.2%	10.2%
48	16.05%	15.3%
60	15.2%	9.1%
72	17.1%	10.03%
84	19.02%	14.3%
96	20.2%	12.2%
108	22.3%	12.1%
120	24.03%	12.3%
132	25.2%	14.1%
144	27.3%	14.2%

Comparative performance analysis

A systematic performance benchmarking exercise was conducted, pitting the proposed hybrid framework against the two abridged variants—one stripped jointly of wavelet denoising and PCA fusion, the other stripped solely of PCA fusion. To provide a clearer picture of how jettisoning key modules affects the fidelity of water-stress detection relative to the proposed hybrid framework, the data are shown in **Figure 11**.

© 2023 The Author(s). | Published by Agro Intelligence Research Press

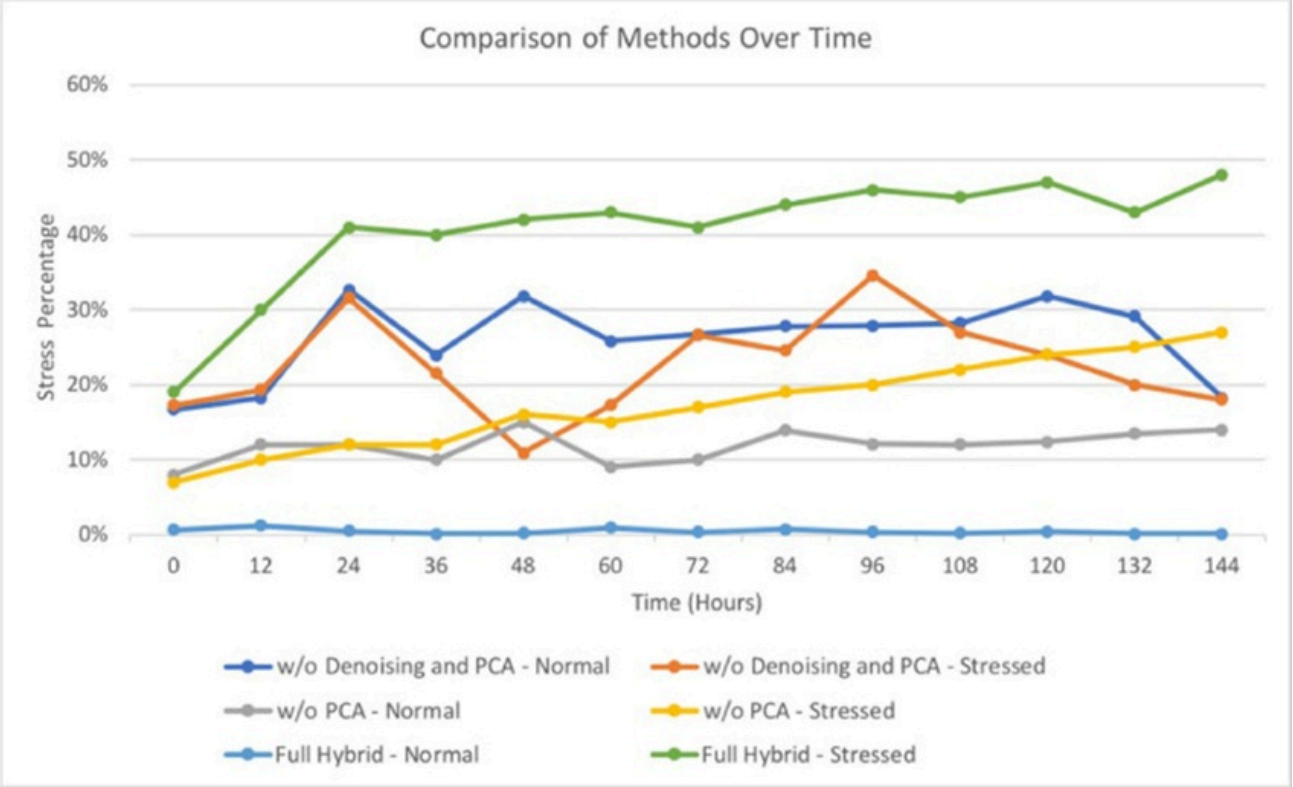

Figure 11. Comparison of methods over time.

The evidence shows that the proposed hybrid framework attains the highest performance ceiling and the greatest consistency, most visibly during the experiment's later hours, when the stressed lettuce canopy undergoes structural alterations. Tossing out both wavelet denoising and PCA fusion begets noisy imagery, erodes detection accuracy, and yields stress zones that fluctuate unpredictably. What is more, discarding PCA fusion alone inflates measurement error because the system loses its grip on canopy structural shifts. As highlighted previously, eliminating PCA fusion alone led to moderate instability due to its inability to accommodate structural changes, in sharp contrast to the high-precision detection delivered by the proposed hybrid framework. This indicates that PCA-based fusion is an indispensable component for reliable water stress detection, given its role in integrating visible and thermal spectral evidence. A condensed synopsis of the comparative analysis is supplied in **Table 8**.

Table 8. Comparative analysis of the hybrid framework over the methods with omitted components.

Metric	Without denoising and PCA	Without PCA	Hybrid framework
Stress percentage accuracy	Inconsistent results	Fault-prone	Consistent performance
Noise level in TIR images	High	Low	Negligible
Stress detection accuracy	Unreliable	Moderate	Highly reliable

Computational time comparison

An efficiency benchmark was performed on the proposed hybrid framework by comparing the time required to handle the full image collection across two platforms: a local IoT board and a remote cloud server via a 5G data link. The Difference Percentage (DP) metric, specified in **Eq. 6**, quantifies the cloud runtime relative to the IoT runtime. The data indicate that running the image batch on cloud resources via a 5G channel took 8.65% longer than local IoT execution.

© 2023 The Author(s). | Published by Agro Intelligence Research Press

$$DP = \frac{|C-I|}{\frac{C+I}{2}} \quad (6)$$

Breaking this down further, performing the workload on the IoT device yielded a 8.27% time savings relative to the cloud-plus-5G arrangement. In comparison, the cloud path imposed a time penalty of 9.02% relative to the IoT baseline, as calculated using **Eq. 7** and **Eq. 8**. **Table 9** lists the abbreviated symbols used in the formulas, along with their corresponding definitions. **Table 10** summarizes the measured metrics for each processing mode—wall-clock durations and the resulting comparative ratios.

$$IP = \frac{C-I}{C} \quad (7)$$

$$ICP = \frac{C-I}{I} \quad (8)$$

Table 9. Table of abbreviations.

Abbreviation	Explanation
DP	Difference percentage
IP	Improvement percentage
ICP	Increase percentage
C	Cloud processing time (seconds)
I	IoT processing time (seconds)

Table 10. Comparison of processing time between IoT and cloud computing.

Metric	Value (%)
Difference percentage (DP)	8.65
Improvement percentage (IP)	8.27
Increase percentage (ICP)	9.02

The body of scientific literature documents that a plant subjected to water shortage mounts its earliest physiological defense by closing its stomatal apertures, thereby limiting the escape of water through transpiration—the evaporative pathway that moves moisture from internal leaf tissues to the ambient air. When transpiration rates or broader metabolic activity decline, leaf surface temperature rises. The hybrid image processing pipeline developed in this work leverages wavelet denoising, PCA-guided fusion, and GMM clustering to capture water stress during this initial phase.

The most consequential observation is that the proposed technique identifies water stress in lettuce specimens within the first 12 hours. In contrast, the capacitive soil moisture probes register their first meaningful decline only after 72 hours. This finding spotlights how the proposed hybrid framework overcomes the well-known shortcomings of soil moisture sensing. Equally noteworthy, the pipeline maintains uniform and trustworthy stress estimates even while the drought-

© 2023 The Author(s). | Published by Agro Intelligence Research Press

exposed lettuce undergoes canopy restructuring—a direct benefit of incorporating wavelet denoising and PCA-based fusion of RGB and TIR image data.

Statistical testing reinforces the dependability of the proposed approach. The strongly significant p-value emerging from the paired t-test confirms the proposed method's clear edge over soil moisture sensors. The tighter dispersion of results from the proposed method further substantiates its superior repeatability in stress detection compared with traditional techniques such as soil moisture probes.

One fundamental constraint—common to every existing methodology and vegetation index and equally applicable here—is the inability of the proposed technique to distinguish water stress from other forms of plant stress, such as those triggered by viral or microbial pathogens. Follow-up investigations might integrate additional IoT sensing hardware operating in alternative spectral windows, such as multispectral or hyperspectral imagers, to merge complementary data streams and sort stress events into biotic or abiotic categories. Additionally, the rapidity of data throughput is essential if corrective actions are to be applied before water stress inflicts permanent damage on the lettuce; the recorded measurements show that processing the image collection on a local device trims computation time by up to 8.27% relative to cloud processing over a 5 G link.

Broader comparative evaluations should be extended to other cultivation contexts, among them vertical farming facilities. The proposed pipeline warrants testing against outputs from diverse camera technologies, including hyperspectral and multispectral instruments. Future comparative research of this kind would help gauge the proposed method's merits and, more expansively, assess its usefulness and operational efficiency across a spectrum of agricultural scenarios. In a related vein, the infusion of Artificial Intelligence (AI) capabilities into the proposed workflow is a compelling direction for further inquiry. AI algorithms could be trained to discriminate among stress triggers—separating water deficit from other stressors—by leveraging the sizable datasets the proposed method generates for supervised model training. The resulting AI engines could subsequently be deployed within real-time observation and decision-support frameworks designed to maximize crop productivity. Future studies should also explore hybridizing the proposed technique with complementary surveillance strategies, such as soil condition or irrigation system tracking, alongside other IoT sensing modalities—including cameras spanning different spectral ranges and Industrial IoT (IIoT) sensors—to widen the scope of plant water stress monitoring.

Conclusion

We have presented a novel hybrid image-processing pipeline for early identification of water stress in lettuce, leveraging the combined power of TIR and RGB imaging. The pipeline interlocks a sequence of sophisticated computational steps: HSV-driven background subtraction, wavelet denoising for interference suppression, PCA-mediated RGB-TIR integration, GMM-based segmentation, and computation of stress area proportion. By zeroing in on the thermal and spectral characteristics of the plant canopy, the method faithfully maps stressed tissue and transforms those maps into operationally useful intelligence about crop health.

The outputs from the proposed method exhibit high fidelity in prompt recognition of water stress in lettuce, compared with the indirect technique of inferring stress from capacitive soil moisture readings. In specific terms, the proposed method can signal water stress up to 84 h in advance. These findings also align with the established literature, which shows that stomatal closure—a consequence of evapotranspiration dynamics—is the earliest detectable symptom of water stress in plants. Furthermore, the rapid turnaround of captured imagery is pivotal to enacting the countermeasures needed to alleviate water stress and resume standard irrigation.

The ablation-style comparison between the complete hybrid framework and variants that omit wavelet denoising and PCA fusion underscores the vital role wavelet denoising plays in suppressing TIR image noise, a prerequisite for faithful GMM clustering. Likewise, stripping away PCA fusion severely undercuts both precision and resilience in stress detection,

© 2023 The Author(s). | Published by Agro Intelligence Research Press

particularly when the lettuce canopy undergoes morphological shifts—precisely because PCA fusion jointly draws on TIR and RGB channels and therefore incorporates evidence from both the thermal and visible domains.

In terms of computational efficiency, the comparison shows that local data processing outperforms cloud-based execution by 8.27%. A supplementary benefit of on-device computation is its straightforward architectural footprint, even while acknowledging the bandwidth limitations inherent to 5G connectivity. Should those communication constraints be overcome, cloud processing could surpass local execution in large-scale rollouts of the proposed method, especially with the emergence of 6 G networks that promise markedly lower latency and higher data rates.

The proposed hybrid framework demonstrates superior scalability and portability across diverse agricultural environments compared to conventional methodologies. Applying wavelet denoising to the TIR stream and PCA to fuse RGB and TIR data enriches the feature space, capturing key stress signatures. Simultaneously, GMM clustering reliably demarcates stress-affected zones, highlighting the framework's potential to refine water stewardship and meaningfully minimize production losses. Beyond this, coupling AI models with the proposed technique could reduce the need for manual inspection and pave the way for automated water-stress diagnostics. Future research efforts should prioritize the development of AI models trained on outputs generated by the proposed method in large-scale indoor farming operations, where real-time analytics and the conversion of data into actionable insights are critical.

Statistical analysis verified that the proposed method outperforms soil moisture sensors in the domain of early water stress detection accuracy. The highly significant t-test result authenticates the method's readiness for greenhouse adoption. The proposed approach represents an effective solution for rationalizing water consumption.

Future investigations should focus on deploying the proposed method across expansive greenhouse installations, leveraging 6G network infrastructure that offers lower latency and faster speeds than current 5G technology. The proposed method's capacity to detect plant water stress promptly is instrumental in reducing both production losses and water waste. Integrating the proposed method into precision irrigation regimes can contribute tangibly to water sustainability objectives.

In summary, the proposed hybrid framework can detect water stress in lettuce with high precision at an early stage. Incorporating this method into a real-time precision irrigation monitoring system can advance water sustainability and boost crop yield.

Acknowledgements

None

Conflict of interest

None

Financial support

This project has received funding from the European Union's Horizon Europe research and innovation programme under grant agreement no. 101135800 (RAIDO).

Ethics statement

None

© 2023 The Author(s). | Published by Agro Intelligence Research Press

Received: 11 Feb 2022 Revised: 18 Apr 2022 Accepted: 04 May 2022
Published online: 25 May 2023

Rights and permissions

Open Access The author(s) retain copyright. This article is licensed under the Creative Commons Attribution-NonCommercial-ShareAlike 4.0 International License. It may be shared and adapted for non-commercial purposes with appropriate attribution, an indication of changes, and distribution of adaptations under the same license. Third-party material may be subject to separate terms identified in its credit line. View the license at https://creativecommons.org/licenses/by-nc-sa/4.0/.

References

1. Hong GZ, Hsieh CL. Application of integrated control strategy and Bluetooth for irrigating romaine lettuce in greenhouse. IFAC-Pap. 2016;49:381–6. https://doi.org/10.1016/j.ifacol.2016.10.070.

2. Fevgas G, Lagkas T, Argyriou V, Sarigiannidis P. Detection of biotic or abiotic stress in vineyards using thermal and RGB images captured via IoT sensors. IEEE Access. 2023;11:105902–15. https://doi.org/10.1109/ACCESS.2023.3320048.

3. Story D, Kacira M. Design and implementation of a computer vision-guided greenhouse crop diagnostics system. Mach Vis Appl. 2015;26:495–506. https://doi.org/10.1007/s00138-015-0670-5.

4. Bendig J, Bolten A, Bennertz S, Broscheit J, Eichfuss S, Bareth G. Estimating biomass of barley using crop surface models (CSMs) derived from UAV-based RGB imaging. Remote Sens. 2014;6:10395–412. https://doi.org/10.3390/rs61110395..

5. Ballesteros R, Ortega JF, Hernández D, Moreno MA. Applications of georeferenced high-resolution images obtained with unmanned aerial vehicles. Part I: Description of image acquisition and processing. Precis Agric. 2014;15:579–92. https://doi.org/10.1007/s11119-014-9355-8.

6. Candiago S, Remondino F, De Giglio M, Dubbini M, Gattelli M. Evaluating multispectral images and vegetation indices for precision farming applications from UAV images. Remote Sens. 2015;7:4026–47. https://doi.org/10.3390/rs70404026.

7. Deery D, Jimenez-Berni J, Jones H, Sirault X, Furbank R. Proximal remote sensing buggies and potential applications for field-based phenotyping. Agronomy. 2014;4:349–79. https://doi.org/10.3390/agronomy4030349.

8. Gonzalez-Dugo V, Hernandez P, Solis I, Zarco-Tejada P. Using high-resolution hyperspectral and thermal airborne imagery to assess physiological condition in the context of wheat phenotyping. Remote Sens. 2015;7:13586–605. https://doi.org/10.3390/rs71013586.

9. Jones HG, Serraj R, Loveys BR, Xiong L, Wheaton A, Price AH. Thermal infrared imaging of crop canopies for the remote diagnosis and quantification of plant responses to water stress in the field. Funct Plant Biol. 2009;36:978. https://doi.org/10.1071/FP09123.

10. Sugiura R, Noguchi N, Ishii K. Correction of low-altitude thermal images applied to estimating soil water status. Biosyst Eng. 2007;96:301–13. https://doi.org/10.1016/j.biosystemseng.2006.11.006.

11. Gao H, Mao H, Zhang X. Inspection of lettuce water stress based on multi-sensor information fusion technology. In: Li D, Liu Y, Chen Y, editors. Comput Comput Technol Agric IV. Berlin, Heidelberg: Springer Berlin Heidelberg; 2011. p. 53–60. https://doi.org/10.1007/978-3-642-18336-2_7..

12. Chandel NS, Rajwade YA, Dubey K, Chandel AK, Subeesh A, Tiwari MK. Water stress identification of winter wheat crop with state-of-the-art AI techniques and high-resolution thermal-RGB imagery. Plants. 2022;11:3344. https://doi.org/10.3390/plants11233344.

13. Yao Y, Liang S, Cao B, Liu S, Yu G, Jia K, et al. Satellite detection of water stress effects on terrestrial latent heat flux with MODIS shortwave infrared reflectance data. J Geophys Res Atmos. 2018;123. https://doi.org/10.1029/2018JD029011.

14. Moreno A, Maselli F, Chiesi M, Genesio L, Vaccari F, Seufert G, et al. Monitoring water stress in Mediterranean semi-natural vegetation with satellite and meteorological data. Int J Appl Earth Obs Geoinform. 2014;26:246–55. https://doi.org/10.1016/j.jag.2013.08.003.

15. Qiu GY, Omasa K, Sase S. An infrared-based coefficient to screen plant environmental stress: concept, test and applications. Funct Plant Biol. 2009;36:990. https://doi.org/10.1071/FP09132.

16. Grant OM, Chaves MM, Jones HG. Optimizing thermal imaging as a technique for detecting stomatal closure induced by drought stress under greenhouse conditions. Physiol Plant. 2006;127:507–18. https://doi.org/10.1111/j.1399-3054.2006.00686.x.

17. Ru C, Hu X, Wang W, Ran H, Song T, Guo Y. Evaluation of the crop water stress index as an indicator for the diagnosis of grapevine water deficiency in greenhouses. Horticulturae. 2020;6:86. https://doi.org/10.3390/horticulturae6040086..

18. Nuruddin MM, Madramootoo CA, Dodds GT. Effects of water stress at different growth stages on greenhouse tomato yield and quality. HortScience. 2003;38:1389–93. https://doi.org/10.21273/HORTSCI.38.7.1389.

19. Mangus DL, Sharda A, Zhang N. Development and evaluation of thermal infrared imaging system for high spatial and temporal resolution crop water stress monitoring of corn within a greenhouse. Comput Electron Agric. 2016;121:149–59. https://doi.org/10.1016/j.compag.2015.12.007.

20. Zubler AV, Yoon J-Y. Proximal methods for plant stress detection using optical sensors and machine learning. Biosens (Basel). 2020;10:193. https://doi.org/10.3390/bios10120193.

21. Pineda M, Barón M, Pérez-Bueno ML. Thermal imaging for plant stress detection and phenotyping. Remote Sens. 2021;13:68. https://doi.org/10.3390/rs13010068.

22. Liao W, Huang X, Van Coillie F, Thoonen G, Pižurica A, Scheunders P, et al. Two-stage fusion of thermal hyperspectral and visible RGB image by PCA and guided filter. 2015 7th Workshop on Hyperspectral Image and Signal Processing: Evolution in Remote Sensing (WHISPERS). 2015:1–4. https://doi.org/10.1109/WHISPERS.2015.8075405.

23. Kaur M, Kaur U. Image analysis of plant stress phenotypes using deep learning and augmented data. 2023 International Conference on Computer Communication and Intelligent Systems (ICCCIS). 2023:206–11. https://doi.org/10.1109/ICCCIS60361.2023.10425563..

© 2023 The Author(s). | Published by Agro Intelligence Research Press